PRAMANA
— journal of
physics

© Printed in India

Vol. 41, No. 6,
December 1993
pp. 525–534

L-dependent heavy ion fusion potentials

S V S SASTRY, A K MOHANTY and S K KATARIA
Nuclear Physics Division, Bhabha Atomic Research Centre, Bombay 400 085, India

MS received 10 May 1993; revised 6 August 1993

Abstract. The energy E and angular momentum l dependence of optical potential for fusion of $^{16}O + ^{208}Pb$ system, observed by Christley *et al* [5], is expressed as a function of radial kinetic energy (ε) instead of explicit E and l dependence. It is shown that the effects of different channel couplings, which result in different effective potentials, can also be parametrized as a function of ε. A correlation is obtained between the energy dependent part of this effective potential and the maximum of the spin enhancement around the Coulomb barrier and both these quantities depend on the details of the channel couplings.

Keywords. l-dependent potential; fusion cross-section; spin distribution; barrier penetration model.

PACS Nos 25·70; 24·10

1. Introduction

The salient features found in the fusion of heavy ions are the enhanced sub-barrier fusion cross-section and the broadening of the compound nucleus spin distribution around the Coulomb barrier which seem to be closely related. The observed sub-barrier fusion cross-sections are not compatible with the predictions of the one-dimensional barrier penetration model (BPM). Earlier studies of sub-barrier fusion enhancement in BPM invoked the influence of orientation of statically deformed reaction partners and of zero point shape fluctuations on the height of potential barrier. In a more general microscopic description, sub-barrier enhancement can be explained by including the coupling to the inelastic and transfer channels. However, one can use a macroscopic model with inclusion of neck degree of freedom which provides an alternate path for fusion process. These dynamical effects of channel coupling or neck opening can be incorporated in an optical model analysis or even in a simple BPM by constructing an effective energy-dependent potential [1, 2]. It has been shown that only energy-dependent effective potential is not consistent with a full dynamical coupled channel calculations [3], unless it depends on both energy E and angular momentum l [4, 5]. It has been shown that [4], the results of a model coupled channel calculation can be reproduced by a simple BPM when the effective barrier height is expressed as function of effective kinetic energy ε, which is the radial kinetic energy at the interaction barrier given by $\varepsilon = E - E_R$ where the rotational energy $E_R = l(l+1)\hbar^2/(2\mu R_b^2)$. Therefore, this simple dependence of the effective potential on ε makes the barrier height (hence the nuclear potential) both E and l dependent. Further evidence for E and l dependent nuclear potential comes from the optical model analysis [5] of fusion for $^{16}O + ^{208}Pb$ system, where the diffuseness

parameter 'a' of the imaginary potential has been varied as a function of both E and l in order to reproduce coupled reaction channel (CRC) results. In § 3 of the present work, it is shown that, diffuseness parameter $a(E, l)$ can also be expressed as a function of ε, instead of an explicit E and l dependence used in [5]. Further, it is shown in § 4 that the effect of different channel couplings (i.e. coupling to inelastic and transfer channels) results in different one channel effective real barrier height which can be parametrized as a suitable function of ε. In other words, a simple parametric form of $V_{\text{eff}}(\varepsilon)$ in BPM can be used to explain the enhancement of fusion cross-section and broadening of compound nucleus spin distribution.

The effective potential can be written as a sum of an energy independent part and an energy dependent part: $V_{\text{eff}} = V_b + \Delta V_p(\varepsilon)$ where ΔV_p can be identified as the polarization potential. In the elastic scattering analysis also one needs a similar energy dependent potential where the strength of the real and imaginary optical potentials show a rapid variation around the Coulomb barrier, known as threshold anomaly [6]. Further evidence shows the strength of the real potential versus energy is a bell-shaped maxima in the vicinity of the Coulomb barrier. In the present case also $\Delta V_p(\varepsilon)$ has a similar behaviour, however instead of energy E it depends on the effective energy ε. The peak of this polarization potential does not necessarily occur at Coulomb barrier, rather it depends on Q value of the non-elastic and transfer channels. In § 5, it is shown that this polarization potential which arises due to various channel couplings, shows a maximum at an energy lower than the Coulomb barrier. However, the effects of these channel couplings on the moments of the spin distribution is maximum at around the Coulomb barrier. It is shown here that the strength of the polarization potential and the spin enhancement around the Coulomb barrier are strongly correlated.

2. The model

The fusion cross-section for a given energy E and partial wave l is written as

$$\sigma_l = (\pi/k^2)(2l + 1)\, T_l(E), \tag{1}$$

where $T_l(E)$ is the penetration probability of lth partial wave at energy E. Using barrier penetration model, it can be written as

$$T_l(E) = 1/[1 + \exp\{(2\pi/\hbar\omega)(V_b + E_R - E)\}], \tag{2}$$

where E_R is the rotational energy, R_b is the position and $\hbar\omega$ is the width of the s-wave barrier. The total fusion cross-section and the average spin value are given by

$$\sigma_f = \sum_l \sigma_l, \tag{3}$$

and

$$\langle l \rangle = \frac{\Sigma l \sigma_l}{\Sigma \sigma_l}. \tag{4}$$

3. L-dependent potential

In an earlier study [4], it was shown that the effects of channel couplings can be introduced by making the barrier height V_b to be energy and l dependent. This was accomplished by parametrizing V_b as a function of ε. Similarly, to reproduce the

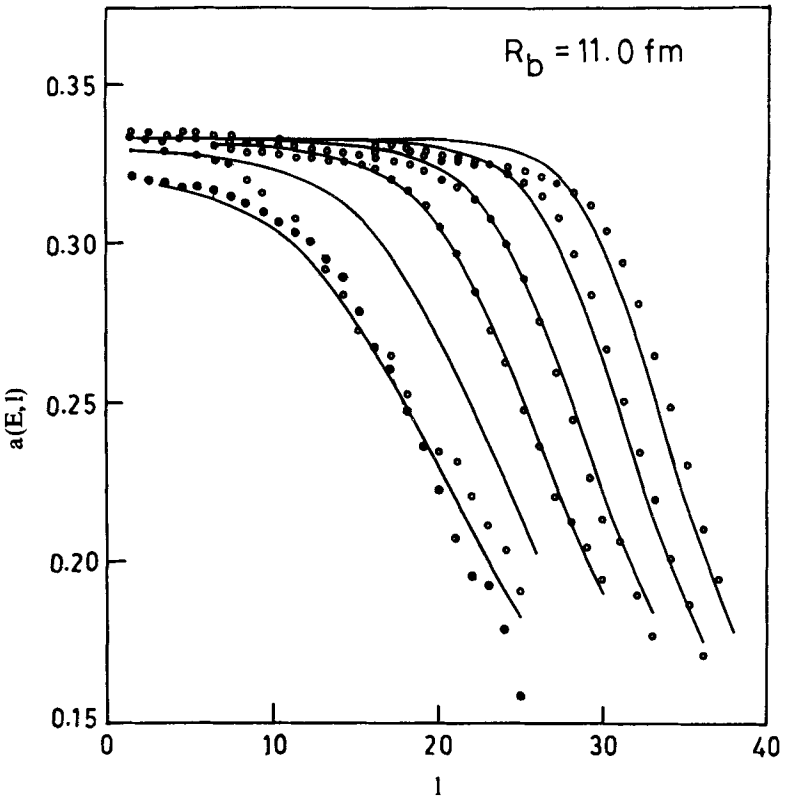

Figure 1. The diffuseness parameter $a(E, l)$ versus l at different laboratory energies from 90, 88, 86, 84, 80 MeV (○) and 82 MeV (●) taken from ref. [5]. The smooth curve is obtained using (9) with parametrization $R_s = 12$ fm, $R_0 = 10{\cdot}38$ fm, $E_e = 72{\cdot}2$ MeV and $a_e = 1{\cdot}4$ MeV.

fusion mean square spin values of $^{16}O + ^{208}Pb$ system is an optical model study, the imaginary potential was expressed as a function of ε [8]. The need to have both E and l dependence has also been studied by Christley *et al* [5], where the diffuseness parameter of the imaginary potential was varied as a function of l. Figure 1 shows the diffuseness parameters as a function of l for different energies E taken from [5]. However, we show here that the observed $a(E, l)$ dependence can also be obtained as a consequence of ε-dependence of the strength of the imaginary potential [8]. In these calculations, the imaginary potential is written as a product of two functions i.e. the radial part $f(r)$ and the ε dependent part $g(\varepsilon)$. Therefore, the imaginary potential is written as

$$W_f(r) = W_0 f(r) g(\varepsilon), \tag{5}$$

and

$$f(r) = 1/\{1 + \exp[(r - R_0)/a_0]\}, \tag{6}$$

and

$$g(\varepsilon) = 1/\{1 + \exp[(E_e - \varepsilon)/a_e]\}. \tag{7}$$

As seen from (7), $g(\varepsilon)$ has an implicit E and l dependence through the variable ε. The value of E_e is very close to the Coulomb barrier. Alternatively, energy and l dependence of $W_f(r)$ can be introduced through the radial diffuseness parameter

$a(E,l)$ as in [5]. In this parametrization W_f can be written as

$$W_f(r) = W_0/\{1 + \exp[(r - R_0)/a_b(E,l)]\}. \tag{8}$$

Comparing the strength of (5) and (8) at strong absorption radius $r = R_s$, we can write

$$a_b(E,l) = (R_s - R_0)/\log[\{f(R_s)g(\varepsilon)\}^{-1} - 1]. \tag{9}$$

The diffuseness values obtained by Christley *et al* [5] (see figure 1) can be reproduced using (9) (solid curve in figure 1) except at 82 MeV with $R_0 = 10{\cdot}38$, $a_0 = 0{\cdot}33$, $E_e = 72{\cdot}2$ MeV and $a_e = 1{\cdot}4$ MeV and $R_s = 12$ fm. The value of Coulomb barrier for this system is 74·6 MeV which is quite close to E_e. These $a(E,l)$ values are also shown in figure 2 as a function of ε for different bombarding energies. For calculation of ε, the value of R_b is taken as 11 fm which is close to the position of the Coulomb barrier. In spite of different E and l dependence of $a(E,l)$ as in figure 1, they all merge into a single curve in ε-scale except for 82 MeV. This data set at 82 MeV does not follow the general systematics with energy and needs to be studied more carefully.

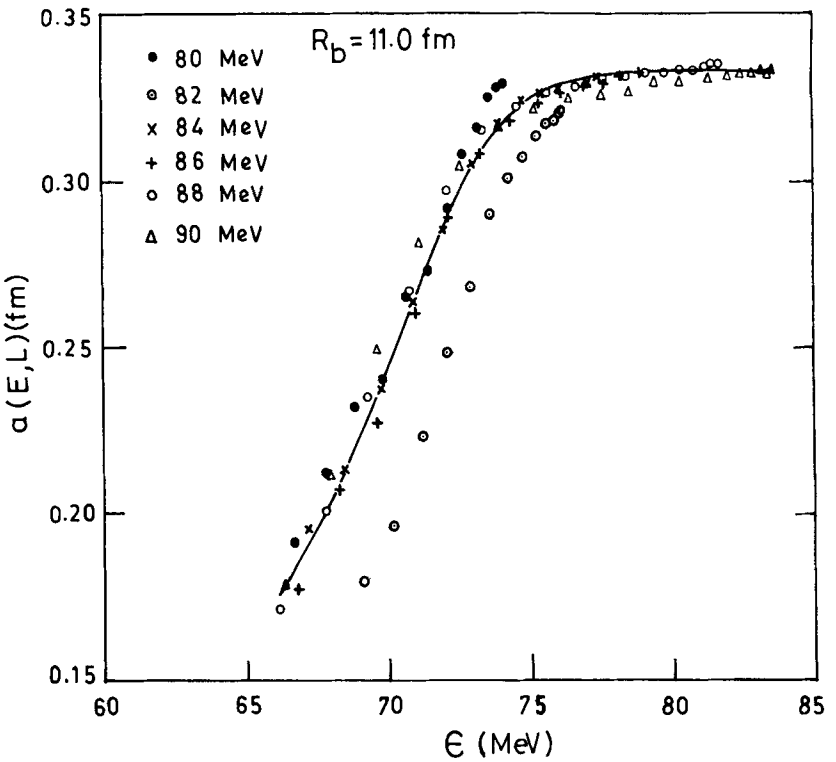

Figure 2. Diffuseness $a(\varepsilon)$ versus ε. The smooth line is the result of parametrization given by (9) as in figure 1. The discrete values with different symbols show the value of $a(\varepsilon)$ for different energies taken for ref. [5].

4. Effective fusion barrier

The effective barrier $V_{\text{eff}}(\varepsilon)$ can be parametrized as [4]

$$\begin{aligned} &\text{if} \quad \varepsilon > E_2 \text{ then } V_{\text{eff}} = V_2 \\ &\text{if} \quad E_1 < \varepsilon < E_2, \text{ then } V_{\text{eff}} = \beta\varepsilon + C \\ &\text{if} \quad \varepsilon < E_1 \text{ then } V_{\text{eff}} = V_1. \end{aligned} \tag{10}$$

In this schematic model, we have two limiting barrier heights V_2 and V_1, known as sudden and adiabatic barriers. The difference $\Delta B = V_2 - V_1$ is shown to be a monotonically increasing function of $Z_T Z_P$ [9]. The magnitude of ΔB reflects the coupling effects in an average way. It has been realized that the direct coupling of various inelastic and transfer processes highly influence the fusion cross-section and the spin distribution. In addition to these single step processes, the multistep coupling processes also contribute significantly to fusion. Therefore, one needs to solve the coupled equations where all these effects are taken into account. On the other hand, when expressed in terms of an effective potential, the various coupling processes affect the adiabatic barrier V_1 significantly. In other words, the effect of adding more channels results in the effective barrier which can be parametrized as some suitable function of ε. In [4], we had considered the couplings to only inelastic states. However, in the present case we consider the effect of positive Q value transfer channels on effective fusion barrier in addition to the inelastic states.

The coupled channel calculations are carried out for $^{58}\text{Ni} + {}^{64}\text{Ni}$ systems using CCFUS code [10]. The dashed curve in figure 3 shows the coupled channel results for fusion cross-sections as a function of energy E_{cm} when coupling to only a few inelastic states are included (2^+, 3^- and 4^+ states of ^{58}Ni and ^{64}Ni). The strength of various inelastic modes are taken from [11]. To find the effective barrier height in BPM which will reproduce the coupled channel results, V_{eff} is calculated by inversion procedure from (1) and (2) as

$$V_{\text{eff}} = \varepsilon + (\hbar\omega/2\pi)\log[(\pi/k^2)(2l+1)/\sigma_1 - 1]. \tag{11}$$

Therefore, knowing l and σ_l from CC calculations, $V_{\text{eff}}(\varepsilon)$ at different bombarding energies is estimated. Figure 4 shows $V_{\text{eff}}(\varepsilon)$ versus ε at two energies; 110 MeV and 100 MeV. It can be seen that irrespective of different bombarding energies, $V_{\text{eff}}(\varepsilon)$ (for different energy E) merge into a single curve. The values chosen are $V_2 = 102$ MeV, $E_2 = 102{\cdot}4$ MeV, $V_1 = 96{\cdot}5$ MeV and $E_1 = 95{\cdot}7$ MeV. The BPM calculation with these parameters results in fusion cross-section shown in figure 3.

As seen in figure 3, coupling to only inelastic channels is not adequate to reproduce the experimental fusion cross-sections. It was pointed out in [11] that it is most likely due to the fact that $^{58}\text{Ni} + {}^{64}\text{Ni}$ combination allows for two neutron transfer reactions due to positive Q value. Accordingly, when coupling strength of 1 MeV is added at $Q = +5$ MeV, it results in the dashed-dot line. The corresponding V_{eff} values are shown in figure 4. Therefore, it can be seen that any additional effects of channel coupling results in lowering of the effective barrier height V_{eff}. In other words, channel coupling lowers the adiabatic barrier V_1 (also E_1), whereas the sudden limit values V_2 and E_2 do not change significantly. Further, the CC results (with inclusion of positive Q value transfer channel) enhance the fusion cross-section. It is not sufficient to reproduce the experimental results as the number of channels included are not

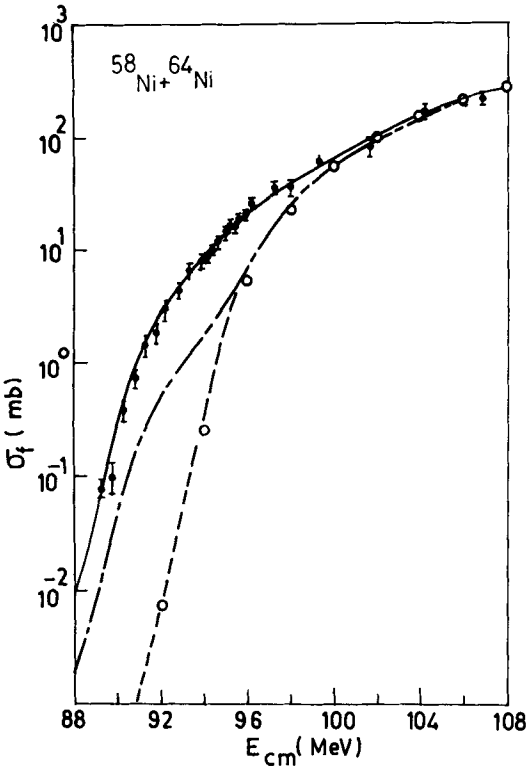

Figure 3. Fusion cross-sections versus E_{cm} for $^{58}Ni + ^{64}Ni$ systems. (– – –) result of coupled channel calculations with inelastic couplings alone. (– · – · –): CC results with transfer channel included. (○) and (———) are the results of ε dependent BPM with the schematic barrier parameters given in figure 4 (smooth line and broken line). The data points are taken from ref. [12].

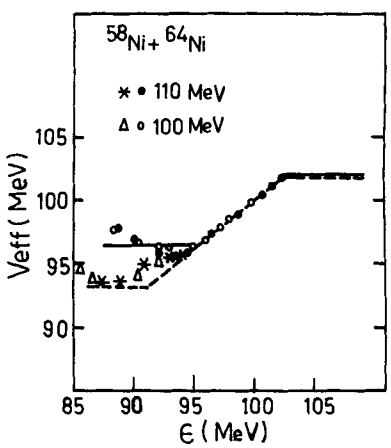

Figure 4. V_{eff} versus ε. The filled and open circles are obtained by inversion from the CC results (with inelastic channels included) using (10) at $E_{cm} = 110$ and 100 MeV. The stars and triangles are the corresponding values with transfer channel included. The smooth and broken lines are two sets of schematic parameters.

adequate and also using CCFUS, couplings to inelastic and transfer channels are considered in an approximate way [11]. However, the new set of parameters i.e. $V_2 = 101{\cdot}6$ MeV, $E_2 = 102{\cdot}2$ MeV, $V_1 = 93{\cdot}2$ MeV and $E_1 = 91{\cdot}2$ MeV results in the smooth curve in figure 3, which fits the experimental fusion cross-section rather well. Comparing the parameters of these two sets, it can be seen that the sudden values of V_2 and E_2 remain more or less same but the adiabatic values V_1 and E_1 are different. The difference between two adiabatic barrier heights is about 3·3 MeV which is quite close to the Q value of two neutron transfer. It is now clear that the effective barrier resulting from inclusion of more and more channels can be parametrized as a function of ε, which is a necessary and relevant parameter for fusion.

Therefore, the schematic model of (10), where the effective barrier height depends on ε, takes into account all the dynamical effects of channel coupling. In the following, we use this model to study the polarization potentials and its effect on the average spin of the compound nucleus, in the vicinity of the Coulomb barrier.

5. Polarization potential and enhancement in spin distribution

Figure 5(a) shows the plot of $\Delta V_p = (V_{\text{eff}} - V_b)$ as a function of ε for $^{58}\text{Ni} + ^{64}\text{Ni}$ system. V_{eff} is calculated using (11) where σ_l is taken from CCFUS. V_b is the barrier height when channel coupling is not present. The energy dependent part of the effective potential i.e. ΔV_p can be identified as the polarization potential at R_b, which arises due to channel coupling. While calculating V_{eff}, we have used l-dependent $\hbar\omega$ given by $\hbar\omega_1 = \hbar\omega_0 + 0{\cdot}0004\, l^2$ as suggested in [4]. In the first case only 2^+, in the second case 2^+ and 3^- and in the third case 2^+, 3^- and 4^+ states of both target and projectile are included and the results are given in figure 5(a). As seen in the figure, the position of the maximum occurs much below the barrier V_b which is around 99·4 MeV and with more number of channels included, the peak value of the polarization potential increases, while the position of the peak moves slightly to the left.

In the earlier studies [9], the $\langle l \rangle_m$ values derived from this schematic model which fits fusion cross-sections are compared with the $\langle l \rangle_{0d}$ values obtained from energy independent BPM with a constant barrier height V_b adjusted to explain fusion cross-sections at high energies. A general feature of this study is that the ratio of $\langle l \rangle_m / \langle l \rangle_{0d}$ shows a peak at around Coulomb barrier and falls to unity on either side. This enhancement is an indication that effects of channel couplings are maximum near the Coulomb barrier. This is in a way similar to the threshold anomaly seen in the optical potential which explains elastic scattering. This effect is not seen in the fusion cross-section data. However, these features are significant in the moments of the compound nucleus spin distributions.

Figure 5(b) shows the value of $\langle l \rangle_m / \langle l \rangle_{0d}$ as a function of energy with different polarization potentials as shown in figure 5(a). Eventhough, the maximum in the polarization potential is to the left of V_b, the ratio of the moments peak at around V_b. However, the height and the width of the ratio depend very much on the strength of the polarization potential ΔV_p. Figure 5(c) shows the plot of the height and width of the enhancement factor as a function of ΔV_p. In this figure, two additional data points are obtained considering the 2^+, 3^- and 4^+ states of either the target or the projectile. The observed correlation suggests that the height of this enhancement can be treated as a measure of the coupling strength and the width as a measure of the region over which the enhancement takes place. It is also evident from figure 5 that the polarization potential peaks left to the one-dimensional barrier height V_b, depend

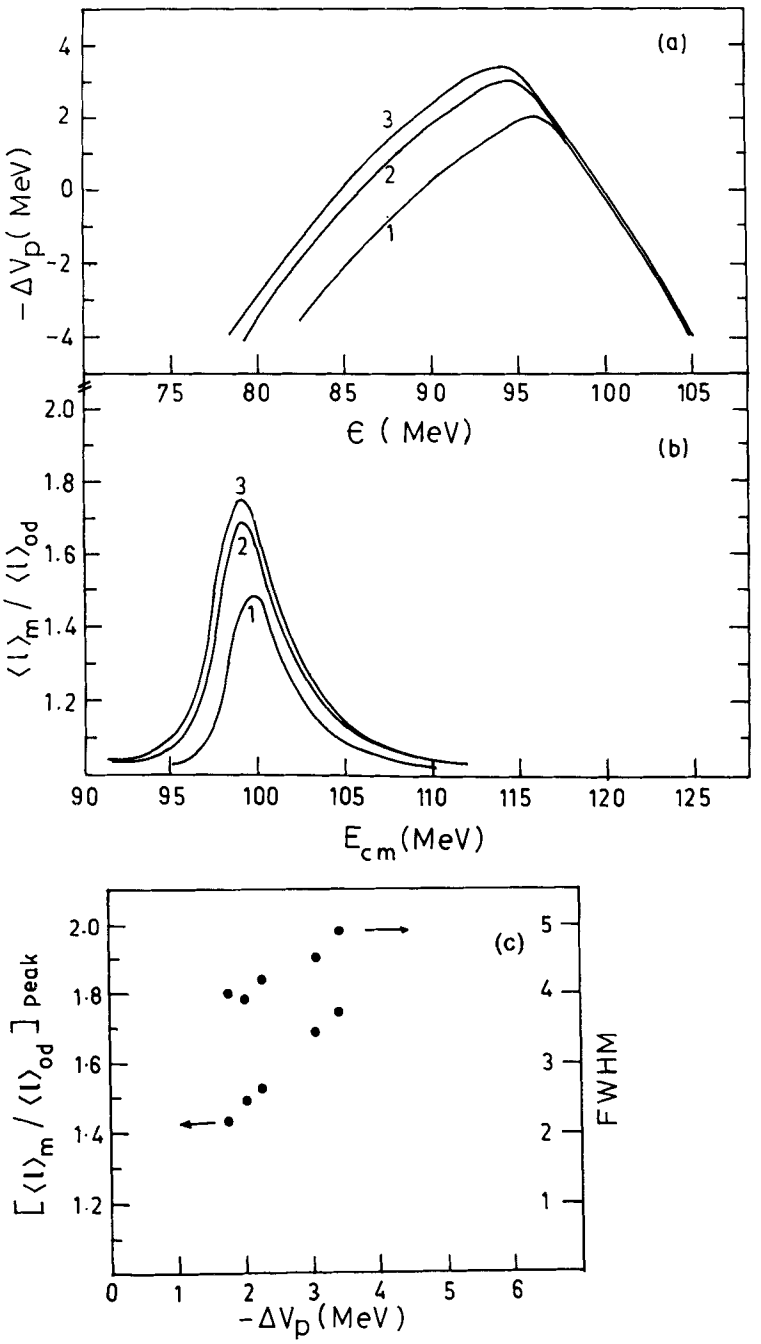

Figure 5(a). ($V_{eff} - V_b$) versus ε for ^{58}Ni + ^{64}Ni system derived from CCFUS with different coupling schemes as described in the text **(b)** $\langle l \rangle_m / \langle l \rangle_{0d}$ versus E_{cm} for ^{58}Ni + ^{64}Ni system with same coupling scheme as figure 5(a). (c) The peak and the width of the ratio $\langle l \rangle_m / \langle l \rangle_{0d}$ as a function of ΔV_p for ^{58}Ni + ^{64}Ni system.

on the Q value of the channel couplings, while $\langle l \rangle_m / \langle l \rangle_{0d}$ peaks around V_b and this peak position does not depend significantly on the details of the channel couplings. However, the height and the width of the ratio depend strongly on the details of the

channel coupling and are model-dependent. Figure 6(a) shows $\langle l\rangle_w/\langle l\rangle_{0d}$ ratio for $^{16}O + ^{154}Sm$ system using Wong's model with three values of β_2 parameter. It can be inferred that the qualitative behaviour of enhancement for these two models (figures 5(b) and 6(a)) are same. In addition to $\langle l\rangle$, another physical quantity associated with fusion spin distribution is its width i.e. the second central moment of the distribution as given by $\Delta l^2 = \langle l\rangle^2 - \langle l\rangle^2$. The channel couplings broaden the fusion spin distribution and this effect can be seen in Δl as compared to its corresponding one-dimensional BPM result. It contains the information as to how many partial waves are effectively influenced by channel couplings. Figure 6b shows the plot of $\Delta l_w/\Delta l_{0d}$ as a function of E for the same values of V_b and β_2 parameter used in figure 6a. It is seen that, as the coupling effects are maximum around V_b, this ratio peaks around V_b. Thus, the channel coupling effects are best illustrated by the moments of the spin distribution. Figure 7 shows the plot of $\langle l\rangle_m/\langle l\rangle_{0d}$ as function of E with different value of V_b. As seen in this figure, the position of the peak also depends

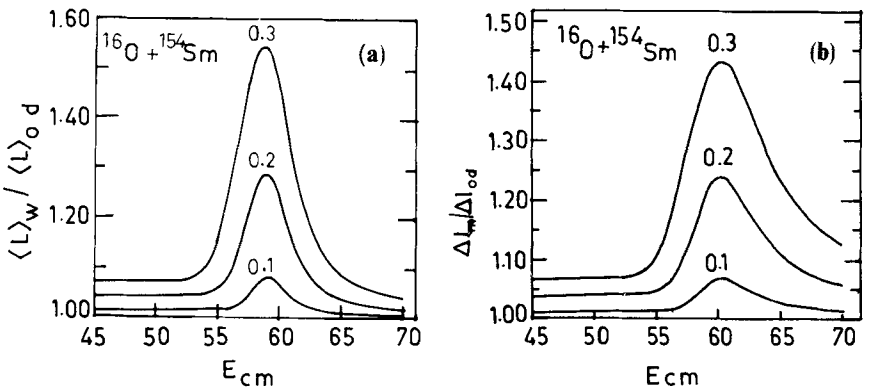

Figure 6(a). $\langle l\rangle_w/\langle l\rangle_{0d}$ versus E_{cm} for $^{16}O + ^{154}Sm$ system where $\langle l\rangle_w$ has been obtained from Wong's model with three deformation parameter (β_2) as shown in figure, (**b**) $\Delta l_w/\Delta l_{0d}$ versus E_{cm} for $^{16}O + ^{154}Sm$ system with three β_2 values.

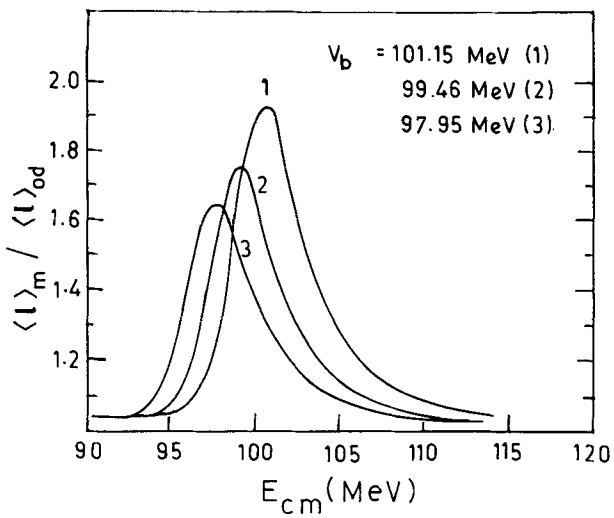

Figure 7. $\langle l\rangle_m/\langle l\rangle_{0d}$ versus E_{cm} for $^{58}Ni + ^{64}Ni$ system with different one-dimensional barrier V_b as shown in figure.

strongly on V_b. However, in reality V_b is taken as one-dimensional barrier height which fits the high energy fusion cross-sections.

5. Summary

In conclusion, the dynamical effects of channel couplings can be incorporated in the optical model or in BPM through the one-channel effective potential which is both E and l dependent. This explicit E and l dependence of the effective potential has been expressed as a function of ε in both the cases. The observed E and l dependence of radial diffuseness parameter $a(E, l)$ in a recent optical model study is a natural consequence of the dependence of imaginary potential on ε parameter. It is also shown that in a BPM, the ε dependent barrier height can reproduce all the effects of channel couplings. The ratio of $\langle l \rangle_m$, obtained from the coupled channel, to $\langle l \rangle_{Od}$ shows a peak around the coulomb barrier and its correlation with the polarization potential has been studied in detail.

Acknowledgements

The authors are thankful to Dr S S Kapoor and Dr V S Ramamurthy for fruitful discussions.

References

[1] C Mahaux, H Ngo and G R Satchler, *Nucl. Phys.* **A449**, 354 (1986); **A456**, 134 (1986)
[2] V S Ramamurthy, A K Mohanty, S K Kataria and G Rangarajan, *Phys. Rev.* **C41**, 2702 (1990)
[3] C H Dasso, S Landowne and G Pollarolo, *Phys. Lett.* **B217**, 25 (1989)
[4] A K Mohanty, S V S Sastry, S K Kataria and V S Ramamurthy, *Phys. Rev. Lett.* **65**, 1096 (1990)
[5] J A Christley, M A Nagarajan and I J Thompson, *J. Phys.* **G17**, L-163 (1991)
[6] Lilley J S *et al*, *Phys. Lett.* **B151**, 181 (1985)
Fulton B R *et al*, *Phys. Lett.* **B162**, 55 (1985)
Baeza A *et al*, *Nucl. Phys.* **A419**, 412 (1984)
[7] J S Lilley, M A Nagarajan, D W Banes, B R Fulton and I T Thompson, *Nucl. Phys.* **A463**, 710 (1987)
[8] A K Mohanty *et al*, *Phys. Lett.* **B247**, 215 (1990)
[9] A K Mohanty, S V S Sastry, S K Kataria and V S Ramamurthy, *Phys. Rev.* **C46**, 2012 (1992)
[10] C H Dasso and S Landowne, *Comput. Phys. Commun.* **46**, 187 (1987)
[11] R A Broglia, C H Dasso, S L Landowne and G Pollarolo, *Phys. Lett.* **B133**, 34 (1985)
[12] M Beckerman *et al*, *Phys. Rev.* **C23**, 1581 (1981)